Ann. For. Sci. 64 (2007) 743–756
© INRA, EDP Sciences, 2007
DOI: 10.1051/forest:2007054

Available online at:
www.afs-journal.org

Original article

Solar activity, global surface air temperature anomaly and pacific decadal oscillation recorded in urban tree rings

Xingyuan HE[a], Zhenju CHEN[a]*, Wei CHEN[a], Xuemei SHAO[b,c], HongS HE[a,d], Yu SUN[a]

[a] Institute of Applied Ecology, Chinese Academy of Sciences, 72 Wenhua Road Shenhe District, Shenyang, 110016, China
[b] Institute of Geographical Sciences and Natural Resources Research, Chinese Academy of Sciences, Jia 11 Datun Road, Beijing, 100101, China
[c] Institute of Tibetan Plateau Research, Chinese Academy of Sciences, 18 Shuangqing Road, Beijing,100085, China
[d] School of Natural Resources, University of Missouri, Columbia, USA

(Received 26 October 2006; accepted 10 May 2007)

Abstract – A tree ring width chronology developed from 58 samples taken from Chinese pine trees (*Pinus tabulaeformis* Carr.) growing in Shenyang city was studied to analyze the effects of solar activity, Global Surface Air Temperature Anomalies (GSATA) and the Pacific Decadal Oscillation (PDO) on annual radial growth. An excellent response of tree rings to solar activity and global environmental change was revealed, indicating that these urban Chinese pine trees are a suitable proxy for Sun-Earth system research despite their location in Shenyang, an industrial city. The information derived from annual growth rings of urban Chinese pine trees coincides with records from undisturbed trees in a natural location, and demonstrates significant synchronous response to solar activity in the periodic bands of 5–8, 10–12 and 20–30 years. The wave signal of tree growth was also affected and amplified by the combined effect of the PDO from 1900 to 2004 and GSATA from 1880 to 2004 with a short lag time, revealing 5–8, 11–13, and 20–23 year oscillatory modes. At 20–30 year timescale, Chinese pines validated the strong GSATA influence signal at 20.8 years, and may be the primary cause of the 20 and 23 year periodic waves of tree rings. Shenyang urban tree ring growth also showed high frequency variation (2–4 y) that may be due to low periodicity of solar activity, GSATA, PDO and local climate variations, especially in the 2–4 years band width.

urban tree rings / sunspot number / Pacific decadal oscillation / global surface air temperature anomaly / wavelet analysis

Résumé – Impact de l'activité solaire, anomalie globale de température de l'air et oscillation décadaire pacifique sur les cernes d'arbres en milieu urbain. Une chronologie de largeur de cernes a été développée à partir de 58 échantillons prélevés sur des pins chinois (*Pinus tabulaeformis* Carr.) poussant dans la ville de Shenyang, afin d'analyser les effets de l'activité solaire, de l'anomalie globale de surface de la température de l'air (GSATA) et de l'Oscillation Pacifique décadaire (OPD) sur la croissance radiale. Cette étude a révélé une forte corrélation entre croissance des cernes et activité solaire d'une part, et changement global de l'environnement d'autre part, indiquant que ces pins urbains permettent des études sur les relations Soleil - Terre, malgré leur localisation dans une ville industrielle comme Shenyang. L'information dérivée de la croissance annuelle des cernes coïncide avec des enregistrements sur des arbres non perturbés dans un environnement naturel. De plus elle révèle une réponse significative synchrone avec l'activité solaire avec des périodes de 5–8, 10–12, et 20–30 ans. Le signal de vague de croissance des arbres a été aussi affecté, amplifié par l'effet combiné d'OPD de 1900 à 2004 et de l'anomalie globale de 1880 à 2004 avec un temps de latence réduit, et des modes d'oscillations de 5–8, 11–13 et 20–23 ans. À une échelle de temps de 20–30 ans, les pins chinois ont validé la forte influence du signal de l'anomalie globale à 20,8 années. L'anomalie globale peut être la cause primaire des 20 et 23 années de vagues périodiques des cernes des arbres. La croissance des cernes des arbres urbains de Shenyang a aussi montré une variation importante de fréquence de 2–4 ans qui est peut-être due une faible périodicité de l'activité solaire, de GSATA, de PDO et à des variations climatiques locales, en particulier dans une période de temps de 2–3 ans.

cernes d'arbres urbains / oscillation pacifique décadaire / anomalie globale de surface de la température de l'air / analyse d'ondes / nombre de taches solaires

1. INTRODUCTION

Broad scale global climate phenomena are affected by solar activities, Pacific Decadal Oscillation (PDO), and global surface air temperature anomalies (GSATA). Then, they affect diverse ecological processes. Solar activity has been broadly studied as a driving force of global climate change [3, 15, 22, 27, 53, 57]. Solar radiation influences atmospheric and oceanic circulations, as well as the biosphere [59]. One of the most important characteristics of solar variability is the sunspot variation in the visible half of the Sun, which is quantified through the sunspot number (SSN) [58].

The PDO is a long-term ocean fluctuation first discovered in sea surface temperature (SST) records of the Pacific Ocean. It is a long-lived El Niño-like pattern of Pacific climate variability[42, 43]. The strength of the variability and persistence of the variability in PDO affect rainfall, temperature and terrestrial ecology systems across broad regions of the globe. The PDO changes every 20–30 years and exerts a great effect on the climate in much of China [43, 67]. PDO variations are often used as a measure of the amplitude of the El Niño/La Niña events [42, 43]. GSATA is derived from global annual-mean

* Corresponding author: chenzhenjuf@163.com

surface air temperature changes recorded by the network of worldwide distributed meteorological stations

Studying the broad scale climate pattern reflected by SSN, PDO and GSATA is challenging because long temporal scales (decades to thousands of years) are involved and historical data is very limited. However, long-lived trees are a viable source for such a study. Tree growth is influenced by various environmental factors, including solar radiation, temperature and precipitation. The width variation of tree rings reflects the influence of environmental factors on tree growth as well as the sensitivity of trees to variations in environmental factors. Tree rings record chronologically and are witnesses of climate and other environment factors that effected tree growth in the past [23, 34, 49, 54, 64]. They make it possible to indirectly monitor variations in solar activity and changes in other geophysical phenomena on relatively long time scales in the past. Studies of the relationships between tree rings and Sun-Earth climatic factors become increasingly common [1, 5–7, 13, 17, 21, 40, 41, 68].

Tree ring data has been used to study solar activity and climate variation in the past [13,20,38,46]. The observed records of the SSN periodicities from growth rings of trees from places with different climates, from satellites and ^{10}Be concentration in polar ice show regular mean cycles near 6, 11, 22, 52 and 90 years in different time scales [2, 19, 20, 24, 33, 38, 46, 47, 51, 52, 63]. These fluctuations are present in centurial and decadal time scales [36]. Other researchers have shown that there is good correlation between solar activity and tree rings [18,33,45,47,51,52], and an 11 year cycle was also found with a short lag time in growth ring series in trees [46]. The variation was commonly monitored through indices constructed from SST and air pressure at sea level [42, 43]. It was also detected by tree rings [14, 16, 17, 35]. Until the present time, temperature reconstruction by tree rings was an essential approach for historical climate study [5, 23, 34, 64]. Temperatures recorded by tree rings comprise an independent archive of past surface temperature change that is complementary to both instrumental records and climate proxies. Local temperature changes are often affected by temperature fluctuations at the hemispherical or global scale [5]. Therefore, research on regional climatic proxies has global significance.

Most of the above investigations are based on trees located in undisturbed regions, far from human living areas. Urban trees have rarely caught researcher's attention because they can be frequently disturbed by anthropogenic factors. However, with rapid urbanization worldwide, studies on urban trees are becoming increasingly important [8,9,31,55,65]. In China, tree ring chronologies studies started in the 1930s [34, 64]. Since then, research using tree rings has been conducted to understand the mechanisms that are responsible for global changes [31,33,56,64]. However, in northeastern China, there has been little research in dendroclimatology, especially in the heavily industrialized cities. It is very difficult to collect enough suitable sample trees in or near those cities. Urban industrial extendibility and rapid population growth have also led to more complicated growing conditions and caused uncertainty about the effects of non-climatic variation between the cities and natural sampling regions.

We analyzed Chinese pine (*Pinus tabulaeformis* Carr.), an endemic conifer species from a well preserved mausoleum dating back to the Ming Dynasty (1368–1644). Trees for this study were located in the suburban old Shenyang of northeastern China (Five thousand pine trees were transplanted from Qianshan Mountain in southern Shenyang in 1643. Twenty-three hundred of these trees have survived to the present day). Chinese pine is among the most important dendrochronological resources for climate reconstruction in China. It forms very distinct annual rings, allowing for confident tree-ring analysis and age determination. The species has a long life (300 to 500 y) and wide distribution in northern China [39]. These reasons make it an ideal material to detect the responses of urban trees to SSN, PDO and GSATA.

The overall objective of this study is to provide evidence that local urban tree growth can effectively capture Sun-Earth variability and activities. We also explore atmosphere–ocean–continental system response to solar variation and the internal oscillation processes in the system. Specifically, we examine (1) the relationships between tree rings and urban climate-environment factors, and (2) relationships between tree rings and the Sun-Earth system as reflected by SSN, PDO, and GSATA. We will also compare our results with those derived from other studies and assess analytical approaches used in this study.

2. MATERIALS AND METHODS

2.1. Sampling site and chronology development

The master ring-width chronology of Chinese pine in Shenyang, Northeast China was the data source for this study on solar and land-ocean climate change. Shenyang (41° 11' 51"–42° 02' 13" N; 122° 25' 09"–123° 48' 24" E; Population: 7.3 million; Area: 8 515 km^2) is an important industrial city, the capital of Liaoning Province and China's fifth largest city. The city lies in the alluvial plains of the Liaohe and Hunhe rivers. Its mean annual temperature is 7.8 °C and the mean annual precipitation is 706.6 mm. The Yellow Sea, Bohai Sea and Pacific Ocean affect the climate in this region. The virgin forests in Shenyang are temperate coniferous and deciduous mixed forests [39]. The conifer studied is a part of the regional vegetation. Urban grown trees in Zhaoling Mausoleum (41° 50' 42"; 123° 25' 45" E; Altitude: 58–64 m, Fig. 1) were used to develop ring-width chronologies. The Mausoleum was constructed during 1643–1651 on 450 ha. It contains a well-known ancient Chinese pine reserve and has been well preserved. It is listed on the UNESCO World Cultural Heritage List. Thirty eight rare and invaluable, ancient, but newly dead, trees and three trees blown down by strong wind were sampled. Two or three increment cores were taken from each of the 39 Chinese pine trees and two time series of tree ring widths were measured on two different directions from each of the two disks in April 2005. These trees had diameter at breast height (DBH) ranging from 35 to 110 cm, and heights ranging from 7 to 18 m. There was no evidence of recent direct disturbance, such as being heavily pollarded, on any sampled trees. Sampling sites were on well drained south facing slopes with meadow brown forest soil. The slope gradient was between 4 and 10%.

Mounted sampled cores and raw disks were fine-sanded with sand paper of decreasing grain size to 600 grit. After adequate polishing,

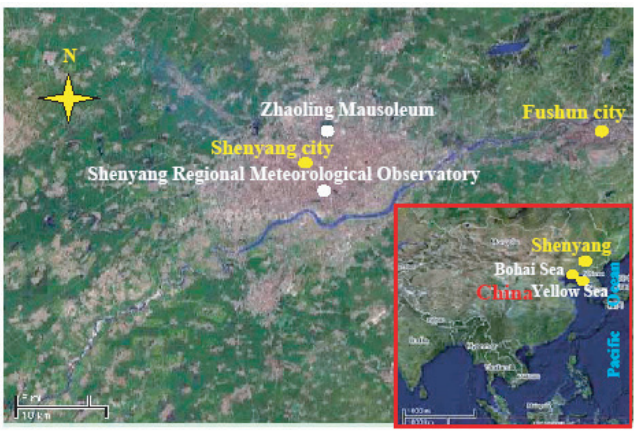

Figure 1. Location of sampling site, Shenyang Regional Meteorological Observatory and Shenyang city in relation to Pacific Ocean (http://treehouse.ofb.net/).

Table I. Information of Master Dating Series from COFECHA.

Quality control and dating check of master dating series	Values
Number of dated series	58
Master series 1706–2004 (years)	299
Total rings in all series	11105
Total dated rings checked	11093
Series intercorrelation	0.570
Average mean sensitivity	0.287
Mean length of series (years)	191.5

all tree rings were visually cross-dated to their exact year of formation using standard dendrochronological techniques [10, 12, 23, 34]. In some cases, the surface of the cross-sections was moistened with drops of water. This increased contrast between early and late wood tissues and improved the distinctiveness of growth zones in general. Ring width was measured to nearest 0.01 mm by a LINTAB5 Tree-ring Measurement and Analysis System. Data was assessed using TASP-Win software. The resulting data set for trees at each individual site was tested for dating accuracy using the program COFECHA [30] (Tab. I). Trees that were not significantly correlated with the mean chronology were excluded. Prior to the analysis, ring-width series were standardized with the program ARSTAN [11]. The detrending procedure was used to remove non-climatic variation, such as a hypothesized negative exponential age-related trend, by fitting a curve to each tree-ring series. This removes most of the low frequency variation, gives dimensionless indices and prevents faster growing trees from dominating the inter-annual variability. Conservative negative exponential and straight-line curve fits [23] were used for this study. Three versions of a master chronology were developed, each with its own inherent characteristics: a Standard chronology (STD), a Residual chronology (RES) and an Arstan chronology (ARS). The STD and ARS retain all frequencies, while the former uses averaged indices and the latter models the communal low frequency and adds it back to the RES. The RES comprises residual indices after prewhitening the STD to remove low-frequency variation. The STD and ARS are usually very similar. However, the ARS can reduce the effects of competition in closed canopy forests [10]. The Zhaoling Mausoleum master chronology was then created using the 26 individual series as the ARSTAN input. All ensuing discussions in this paper are based on

Table II. Statistics for the STD from ARSTAN.

Quality control\Chronology type		Standard
Chronology time span		1706–2004
Total no of years		299
Mean		0.9865
Median		0.922
Mean sensitivity		0.1775
Standard deviation		0.2046
Skewness		–0.2044
Kurtosis		0.0453
Autocorrelation or		0.4535
		Detrended series
Mean correlations	Among all radii	0.354
	Between trees (Y variance)	0.340
	Within trees	0.600
	Radii versus mean	0.689
Signal-to-noise ratio		9.277
Agreement with population chronology		0.903
Variance in first eigenvector (%)		38.02
Chron common interval mean		0.981
Chron common interval std dev		0.196
Subsample signal strength [62] (SSS) ⩾ 0.75		1766–2002 (C*),7 trees
	SSS ⩾ 0.80	1774–2001 (C*), 9 trees
	SSS ⩾ 0.85	1779–2000 (C*), 12 trees
	SSS ⩾ 0.90	1817–1997 (I**), 20 trees

Common interval time span 1846–1988, 165 years, 18 trees, 42 radii. C*: Continuous; I**: interrupted.

the Standard version (Tab. II, Fig. 2) of this chronology. The first year of this version the EPS (Expressed Population Signal) and RBAR (average correlation between trees for the common overlap period among series) [11] are acceptable and reliable is 1733 (Fig. 2B). In this case, RBAR is 30 years long. EPS is a similar parameter for the agreement between trees or common variance in relation to total variance. An EPS over 0.85 is a generally acceptable threshold for reliable chronologies [4].

2.2. SSN, PDO, GSATA and extreme climate year data

The SSN time series (1700–2004) were obtained from the National Geophysical Data Center, USA Web site. The PDO time series (1900–2004) were obtained from Web sites of NOAA and the University of Washington, USA. The GSATA time series (1880–2004) were obtained from the National Aeronautics and Space Administration, USA Web site. Significant El Niño events (1900–2000) were obtained from the University of Illinois at Urbrana-Champaign, USA Web site. Significant La Niña events (1900–2000) were obtained from, Australian Bureau of Meteorology. The local meteorological records (1951–2003) were obtained from the Regional Meteorological Observatory of Shenyang (Fig. 1). The extreme drought year records were obtained from local archives [61].

2.3. Morlet wavelet and Discrete Fourier transform spectrum analysis

A complex Morlet wavelet [49, 60] was used in this work because it is most adequate to continuously detect variations of periodicities in geophysical signals [37]. It was also successfully used in previous

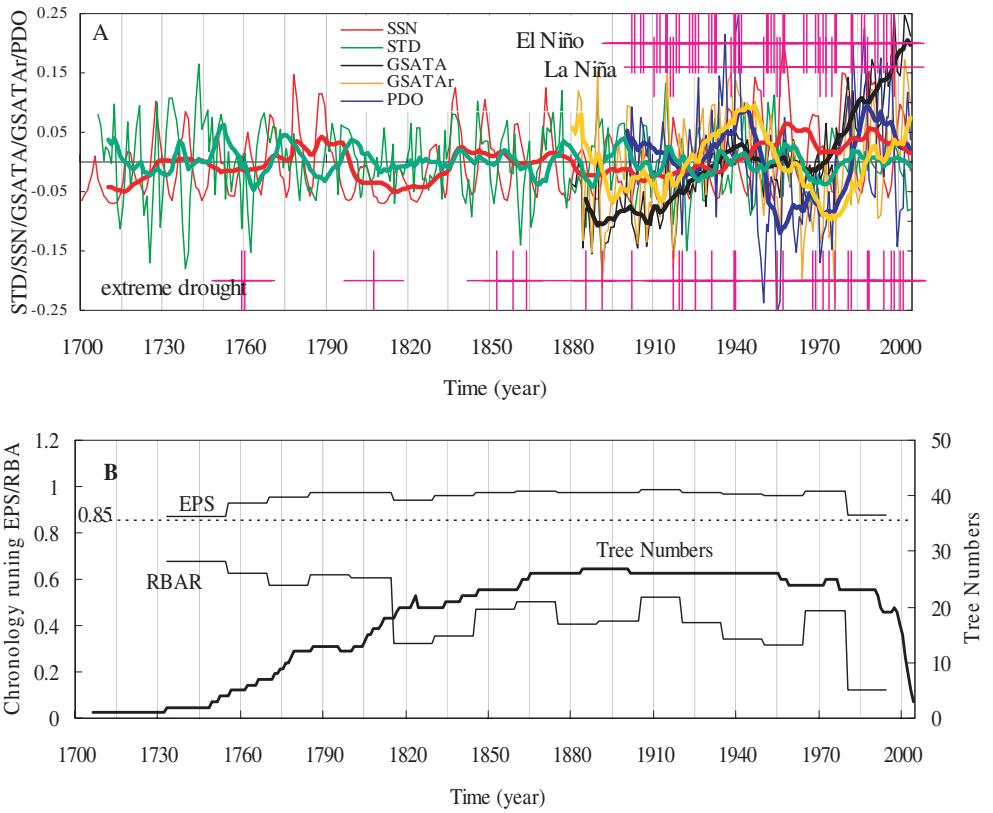

Figure 2. (**A**) STD (1706–2004, thin green curve), SSN (1700–2004, thin red curve), PDO (1900–2004, thin blue curve), GSATA (1880–2004, thin grey curve), and GSATAr (1880–2004, thin brown curve) is the GSATA, which the noise of global surface air temperature increasing trend has been removed by nonlinear regressive multinomial: $\Delta T = 5E-05t^2 - 0.0011t - 0.2183$, t is the dependent variable of temperature anomaly, t is the independent variable of time, for convenient to calculate, t = [1:1:125], $R^2 = 0.6865$; thick curve is 11 years moving averaged of its thin same color curve; Thin vertical lines indicate El Niño events, (b) La Niña events, and extreme drought events in the local region; For convenience to plot and compare, all above time series have been standardized by the function: $Y_i = \frac{X_i - \overline{X}}{\sqrt{\sum_{i=1}^{n}(X_i-\overline{X})^2}}$, i=1, 2, 3, ... n; (**B**) STD running EPS/RBAR, and the sample depth.

research [9, 17, 33, 47, 51, 52]. Pearson correlation analysis was used to detect linear correlations in the time series variability. Cross correlation analysis was also used with wavelet cross spectrum analysis to detect inter-correlations in research objects. The Discrete Fourier transform was used to look for the periodicities embedded in tree growth rings and to detect sensitivity of our STD by Sun–Earth comparison sources [9].

3. RESULTS

3.1. Chronology characteristics and their relationship with local climatic variables

The chronological data obtained in tree ring width standard chronology (STD) from 1706–2004 is analyzed in this paper. The wavelet spectrum for STD reveals strong signals of cyclic oscillation modes, including a relative regular 2–3 year periodic band scattered throughout the whole period. The oscillation has relatively high intensity and significance in some short periods (Fig. 3A). The 6–11 year periodicity, with several short weak intervals (1785–1802, 1862–1885, 1968–1995) in the full time range, is the second strongest band. The amplitude near an 11 year cycle with high intensity appears between 1710–1753 (the highest intensity between 1720–1741, 1830–1857, 1889–1931 and 1934–1953). The two strongest bands with several very short time intervals (near 1836 and 1845) are connected (without obvious time intervals and with a strong 20 year periodicity among them) in the full time range. A 49.8 year cycle (near the 0.05 confidence level) was also observed.

The bivariante correlative analysis between STD and local climate variables shows a significant correlation, especially in the cold season (November to February) and growing season (April to October) despite the Chinese pine at this sample site being heavily affected by urban development, air pollution and other anthropogenic disturbances (Fig. 4A) [31,55,65]. In one example, between 1906 and 1994 (Shenyang urban industries developed greatly, especially after 1950), mean annual air temperature had a slightly higher correlation with ring width in 1906–1950 ($r_{1906-1950} = 0.130$, $p_{1906-1950} = 0.396$) than in 1951–1994 ($r_{1951-1994} = 0.117$, $p_{1951-1994} = 0.446$). The

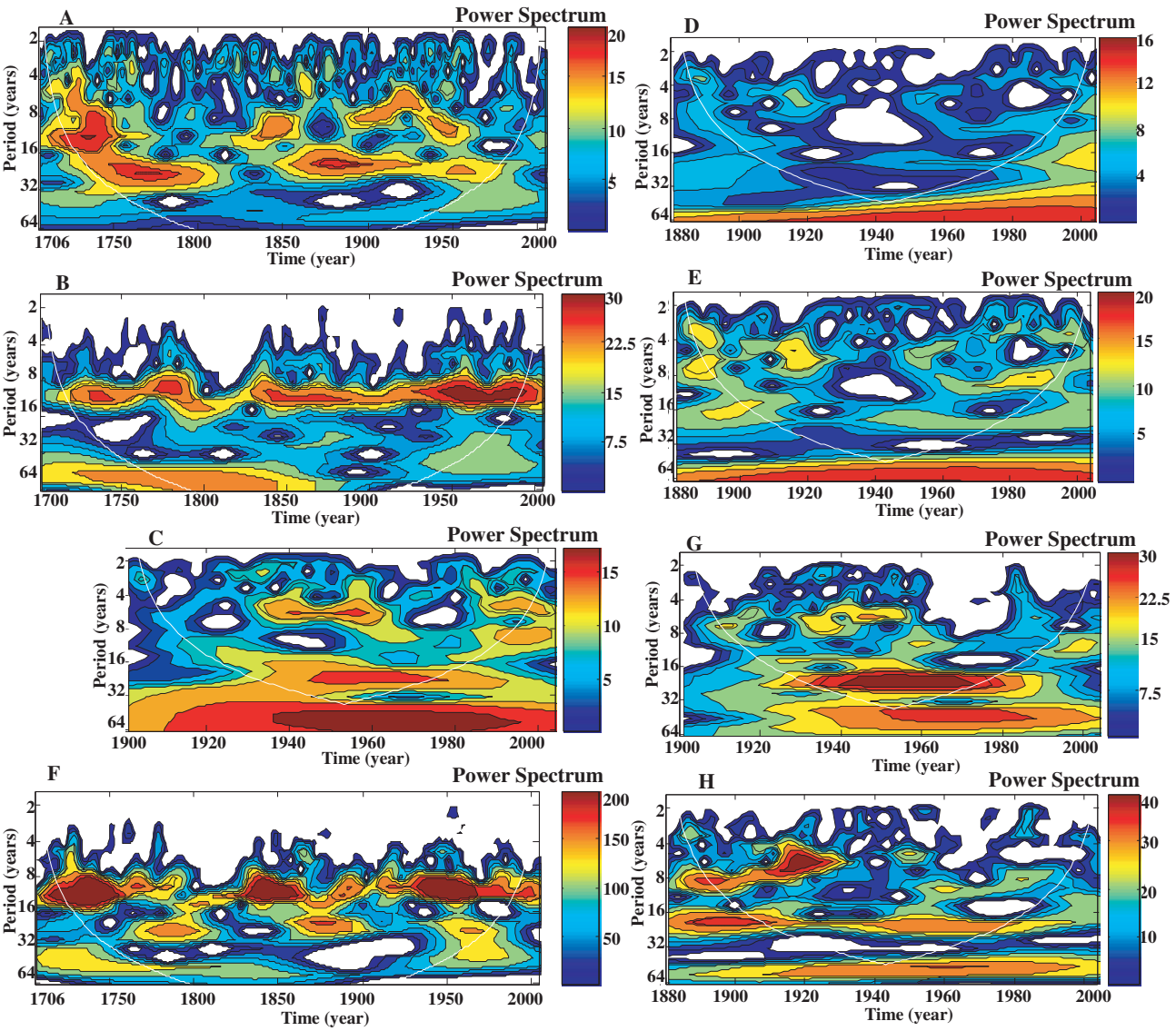

Figure 3. The wavelet spectrum of time series, smooth curve is significance levels contour for 95%. The legend at right side indicates the wavelet spectral power in Jet levels, **(A)** STD; **(B)** SSN; **(C)** PDO; **(D)** GSATA; **(E)** GSATAr (noise removed); **(F)** Cross-Wavelet Spectrum (CWS) between SSN and STD (1706–2004); **(G)** CWS between PDO and STD (1900~2004); **(H)** CWS between GSATAr and STD (1880–2004).

cross-correlations of STD and local climate factors are also significant (Tab. IIIB).

3.2. Relations between local climate and large scale climatic and environmental factors

The local climate was strongly influenced by PDO, GSATA and SSN from monthly to yearly time scales as detected in this research. Results for November to February (Fig. 4B) are presented. The profile of the cross correlation function (Fig. 5) establishes the consistency of the periodic signals. Those signals are common to the STD and an influence (PDO, GSATA or SSN) over numerous lags, suggesting common periodic fluctuations. Our analysis shows that the yearly local mean temperature and yearly local precipitation, the two dominant local meteorological parameters, have synchronous and significant correlations and periodic responses to PDO, GSATA and SSN (Tab. IIIB). SSN mostly affected the local water regimes, including evaporation in May ($r = 0.350$, $p < 0.05$), July ($r = 0.374$, $p < 0.01$), August ($r = 0.435$, $p < 0.01$), September ($r = 0.289$, $p < 0.05$) and October ($r = 0.448$, $p < 0.01$), precipitation in August ($r = -0.280$, $p < 0.05$), and December ($r = 0.385$, $p < 0.01$), as well as relative humidity in August ($r = -0.297$, $p < 0.05$). PDO also has more influence on the local water regimes (such as relative humidity, evaporation, water vapor pressure and precipitation) than temperature factors in the study area (Fig. 4B). GSATA as one dominant factor of global climate change has a great impact on local climate variations, especially for temperature parameters (Fig. 4B).

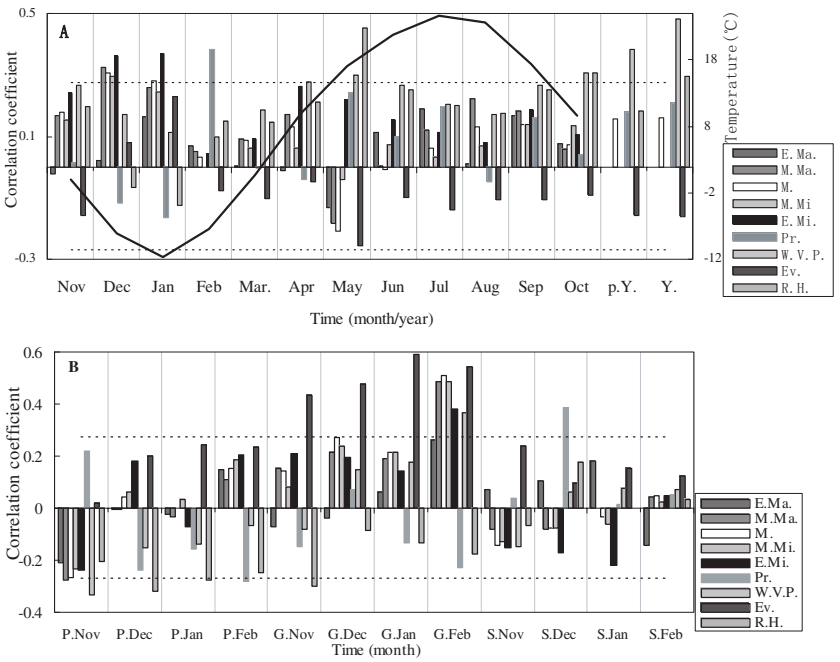

Figure 4. (A) Correlations between STD and local meteorological data (1951–2003). P.Y. is prior year and Y. is growth year. The curve is monthly fluctuations of mean local air temperature in a year (1951–2003). **(B)** Correlations between local meteorological data and PDO, GSATA and SSN, respectively (from November to February, P. is correlation with PDO, G. is correlation with GSATA, S. is correlation with SSN). The dashed lines represent confidence level (95%), and histograms are confidence coefficients in each plot. E.Ma. is extreme maximum temperature, M.Ma is mean maximum temperature, M. is mean temperature, M.Mi is mean minimum temperature, E.Mi. is extreme minimum temperature, Pr. is precipitation, W.V.P. is water vapor pressure, Ev. is evaporation and R.H. is relative humidity.

Seventy one percent of extreme local drought years occurred in El Niño and La Niña years. The evident La Niña events and extreme local drought show similar coincidence with cold PDO and GSATA periods, and 58% of those evident La Niña years (1900–2004) resulted in narrow to extremely narrow annual trees rings (Fig. 2A). Our study also shows that most evident El Niño (above 65%) and La Niña events (50%) took place in lower SSN years and nearly 60% of extreme droughts occurred at SSN wave crests (Fig. 2A).

A strong relationship was observed between the wavelet spectral amplitude and correlations of each two of the three influencing factors from cross-wavelet spectral analysis [9], scale-averaged wavelet power over the 2–8 year band analysis [9], and relative correlation analysis. In this study, monthly GSATA shows significant responses to SSN (mean $r_{Jan-Dec}$ = 0.251, $p < 0.01$, $n = 100$), and SSN also heavily influences PDO, especially in November and December. Therefore, monthly SSN has significant effects on PDO (after 11 years running mean) in November (mean $r_{Jan-Dec} = -0.334$, $p < 0.01$, $n = 120$) and December (mean $r_{Jan-Dec} = -0.371$, $p < 0.01$, $n = 120$). The periodicities of PDO, GSATA and Chinese pine growth are affected by the fluctuation of SSN (Figs. 3 and 6).

3.3. Relations between tree-ring width chronology and SSN

Annual SSN correlates significantly with the derived STD ($r = -0.128$, $p < 0.05$, $n = 299$) from 1706 to 2004. In the period 1940–1990, SSN has very high amplitudes, indicating a very high sunspot number (Fig. 2A). In periods 1830–1870 and 1720–1800 high amplitudes were also observed. The amplitudes in 1940–1990 were high, but less than in the first two periods (Fig. 2A). In these three high amplitude periods, trees showed more significant responses to SSN ($r_{1830-1870} = -0.258$, $p = 0.103$, $n = 41$; $r_{1720-1800} = -0.252$, $p < 0.05$, $n = 81$; $r_{1931-2004} = -0.274$, $p < 0.05$, $n = 74$) than during other periods. Furthermore, the average yearly SSN is 41.8 in 1806–1905, and the correlation between tree ring widths of Chinese pine and SSN in this century is weakest among the past three centuries (1700–2004). In periods 1706–1805 and 1906–2004, average yearly mean SSN is 46.5 and 64.2, respectively, and the correlation between tree ring width and SSN becomes stronger (Fig. 7A).

The wavelet spectrum for the SSN (Fig. 3B) is the strongest for the 8–14 year periodicity (Tab. IIIA) and persistent during the entire period. There is a higher intensity in the 1940–1990 period. A strong low-frequency signal indicating an approximate 50 year cycle (significant at 57.9 y, Tab. IIIA) is persistent throughout the entire period with a short time interval. The signal is stronger in the period of 1700–1868. At the same period, a discontinuous and relatively weak signal is found at approximately the 20 year period (16 y, 28.8 y, Tab. IIIA). Several weak, high-frequency signals were close to the 4–6 y cycle (Tab. IIIA). High-frequency signals occurred around the years 1780, 1838, 1869, 1954 and 1980. This pattern indicates the SSN series' non-stationary behavior.

Table III. (A) STD dominative periodicities and their possible influencing periodicities from other factors (at the 95% confidence level [32]). **(B)** Lag time of cross correlation at confidence level (20 y maximum number of lags in length) between local climate factors and SSN, GSATAr, PDO and STD, respectively. Unit: year.

(A)	Significant periodicity					
Significant periodicity band	SSN	PDO	GSATAr	STD	LP	LT
2–3 yrs	2.1, 2.3, 2.9, 3.3, 3.6, 3.7, 3.9	2.2, 2.8, 3.3	2, 3.4, 3.8	2.1, 2.2, 2.4, 2.5, 3, 3.1, 3.4	2.2, 3.5, 3.8	2.2, 2.3, 3
4–5 yrs	4.1, 4.4, 4.8, 4.9, 5, 5.1, 5.2, 5.8, 5.9	4.3, 4.7, 5.5, 5.8	4, 4.2, 5.2	4.7, 4.9		4, 4.9
6–8 yrs	6, 6.9, 7.2, 7.4, 7.8, 8, 8.2, 8.5, 8.7	8.7		6.4, 7.1, 8.5	8.2	
9–13 yrs	9.3, 9.6, 9.9, 10.7, 11.1, 12, 12.5, 13.1, 13.7			11.1, 11.5, 13		12.3
16–30 yrs	16, 28.8		20.8	19.3, 23		
40–60 yrs	57.9	52	62.5			49
> 70 yrs	96				98	
(B)	SSN	PDO	GSATAr	STD		
LT	-19∼-17, -10∼-6, -4∼-1, 1∼4, 6∼9, 11∼14, 17∼20	-15, -14, -8∼-5, -3∼-1, 8, 9, 11∼13, 17	-8∼-4, -2∼2, 7∼9, 20	-15, -13, -12, -9, -7, -4∼-2, 1, 10∼14, 19, 20		
LP	-20∼-19, -14, -11∼-8, -6∼-3,1, 4–8, 12,17∼19	-17∼-15, -13, -10, -7, -4, -1, 5, 6, 14∼17, 19	-18∼-12, -8, -7, 0, 4, 6, 12∼15, 18∼20	-14, -9, -8, -6, 2∼4, 6∼8, 17, 18		

LP: local yearly precipitation; LT: local yearly mean temperature.
Top 10 powers of significant periodicities in each group:
STD: 20 y > 11.5 y > 13 y > 11.1 y > 8.5 y > 23 y > 7.1 y > 6.4 y > 2.4 y > 4.9 y;
SSN: 11.1 y > 9 y > 96 y > 12 y > 10.7 y > 57 y > 8 y > 28.8 y > 9.6 y > 13.7 y;
PDO: 52 y > 5.8 y >8.7 y > 5.5 y > 3.3 y > 4.7 y > 4.3 y > 2.1 y > 2.9 y;
GSATAr: 62.5 y > 20.8 y > 5.2 y > 4 y > 4.1 y > 2 y > 3.8 y > 3.4 y;
LP: 3.5 y > 98 y > 3.8 y > 8.2 y > 2.2 y;
LT: 49 y >12.3 y > 4.9 y > 3 y >2.2 y > 2.3 y > 3.9 y.

The scale-averaged wavelet power over all scales between 2 and 8 years (Fig. 6A) shows a distinct variation of tree ring width and SSN between 1706 and 2004. During that time, tree ring width variance follows the trend of SSN variance, showing a near 20 year modulation. The response of tree ring width to SSN oscillation has a short time (1–2 y) lag (Fig. 5A), and the lag effect may amplify the influence of SSN on trees. Both time series show consistent interdecadal changes and a low wavelet power interval between approximately 1770 and 1925. The cross-wavelet spectrum plot (Fig. 3F) presents a continuous high amplitude for the periodicity near 11 years in almost the whole period with several weak signals indicating short time intervals (highest near 1750, 1850 and 1950, approximately). Their common periodicity fluctuated from 6 to 16 years in the whole period. The second band of cross-wavelet spectra of SSN × STD has the periodicity near 20 year cycles. The significant intervals are shown in 1750–1825, 1850–1910 and 1925–1988. During these periods, the highest intensity of STD periodicity is at a 23 year cycle (Fig. 3F). This is validated by its significant cross-correlation with SSN at ± 23 years lag time (Fig. 5A). The near 50-year common low frequency signal for the whole range 1706–2004 has an interval from 1807 to 1928.

3.4. Relations between tree-ring width chronology and PDO

It is possible to compare accurately PDO and STD for a more recent epoch. PDO has shown lower amplitudes in cold periods during 1900–1924 and 1944–1977, and relatively higher amplitudes during warm periods in 1925–1943 and 1978–2004. STD has no significant interannual linear correlations with PDO. However, after applying an 11 year moving average, STD was found to have a significant response to PDO in the growing season (May–October) (Tab. IV). Tree ring width in Chinese pine shows more significant response to the PDO in warm periods than to the cold periods (Fig. 7B); suggesting a rhythmic behavior of this response. High values are in the 4–8 year periodicity band during some warm periods 1927–1958 and near 1988 (Fig. 3G), near the 11 year band (12 and ± 13 y lag time cross correlations are significant, Fig. 5B) during 1907–1936, 1949–1975, 1982–present, near 20 years periodicity band and near 50 years periodicity band. The two most significant bands are near the 20 year band and near the 50 year band, which persist over the whole time range. Two strong tree rings, one near 20 year cycles (signal at 20 and 23 years, Tab. IIIA) and one near the 50 year band (49.8 y cycle) can be observed. The 20 year band may be a possible link to sextuple a 3.5 year strongest cycle of local precipitation (6 ×3.5 years = 21 years ≈ 20 years), and duple a 12.3 year strongest cycle of local temperature (2×12.3 years = 24.6 years ≈ 20 years). Other bands also have these evident relationships with local climate cycles (Tab. IIIA). In addition, during the urban industrial period of great development (1900–2004), the correlations between STD and PDO were changed ($r_{1900-1950} = 0.132$, $p_{1900-1950} = 0.355$; $r_{1951-2001} = 0.034$, $p_{1951-2001} = 0.812$).

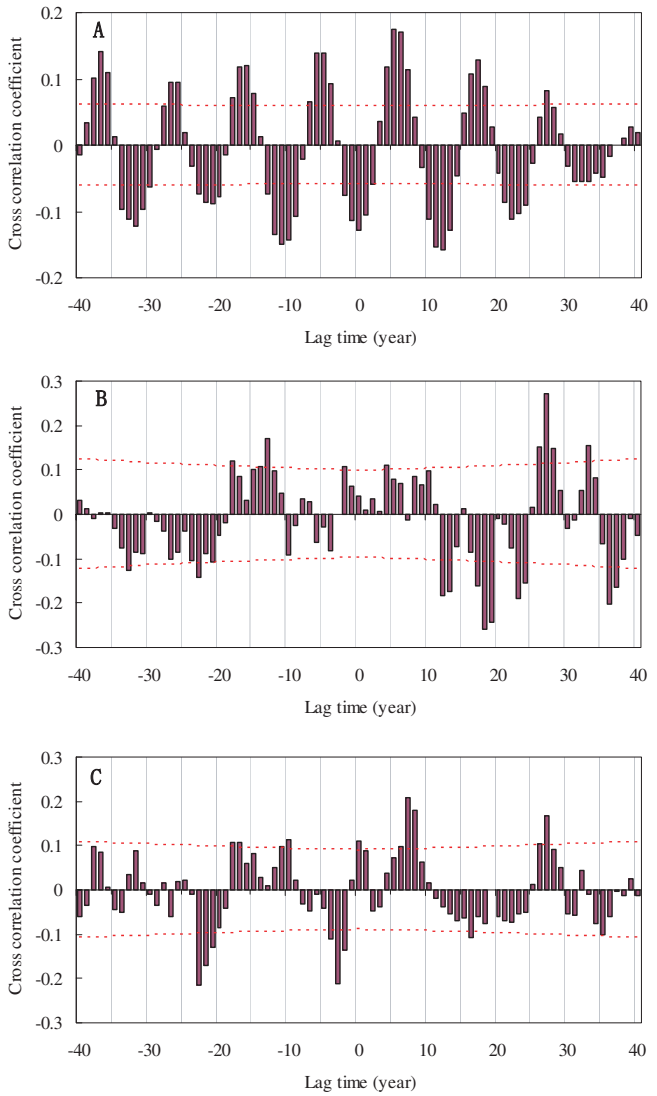

Figure 5. Cross correlations between STD and SSN of 1706–2004 **(A)**; STD and PDO of 1900–2004 **(B)**; STD and GSATA of 1880–2004 in which the noise of global surface air temperature increasing trends has been removed **(C)**. The dashed curves in each plot are confidence limits (standard error limits), histograms are correlation coefficients and vertical dashed lines are calibration tails.

Similar to SSN, PDO has more influence on local water regimes than large scale temperature parameters. The tree ring width is most affected by water regimes (Fig. 4A). In Figure 3C, strong amplitudes are shown around the 2–8 year periodic band during 1939–1959 and the 16–32 year band during 1944–1978 (strongest periodicity is at 26 y. Tab. IIIA). A strong low frequency signal of 50–70 years' cycles (significant at 52 y) also exists. All the signals are non-stationary with alternating periodicities present in some periods but absent in others. The result agrees with the report that the PDO shows several periodicities such as 15–25 years and 50–70 years during 20th century with an increase in frequency in the last decades [26, 42, 43].

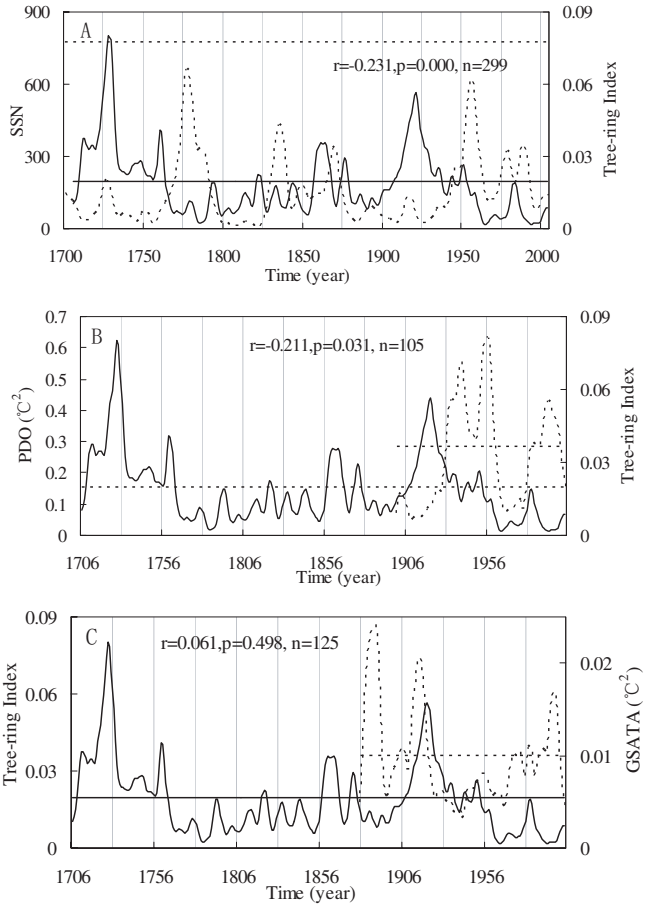

Figure 6. Scale-averaged wavelet power over the 2–8 year band. **(A)** for the SSN (dashed curve) and STD (solid curve). **(B)** for STD (solid curve) and the PDO (dashed curve). **(C)** for STD (solid curve) and the GSATA (dashed curve). Corresponding the solid and dashed curves in each plot, the solid and dashed lines indicate 95 percent confidence level of STD, SSN, GSATA and PDO, respectively.

3.5. Relations between tree-ring width chronology and GSATA

Initially, our results showed no significant interannual linear correlation between STD and GSATA. The increasing trend of earth surface air temperature is reflected as a low-frequency signal in the GSATA time series (Fig. 2A). We removed the red noise and identified two main warm periods and two main cold periods in the time series to show high frequency signals clearly, similar to those found for PDO (Fig. 2A). GSATA's cold periods were in 1880–1918 and 1956–1978, and warm periods were in 1919–1955 and 1979–2004. Prior to 1880, there was a warm period with higher amplitudes. The red noise disturbed long term annual correlation between GSATA and tree rings, and showed an unclear relation between GSATA and STD, even after 3, 5 or 11 years running mean. The relationship of GSATA to local climate variables is also weaker than that with red noise removed. STD results show a more significant response in cold GSATA regimes than in warm GSATA regimes (mean $GSATA_{1881-1920}$ is –0.0257 °C,

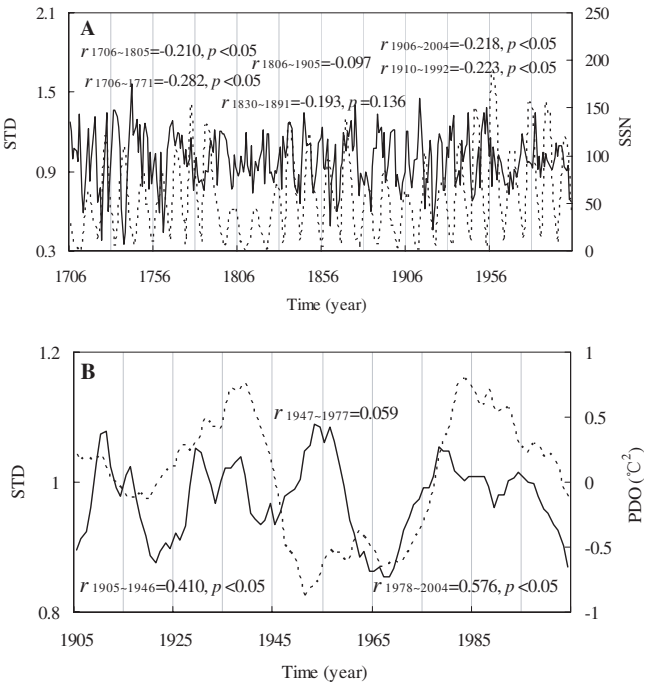

Figure 7. (A) Correlation between STD (solid curve) and SSN (dashed); **(B)** Correlation between STD (solid line) and PDO (dashed) (after 11 years running mean).

$r = 0.230$, $p = 0.154$; mean $GSATA_{1921-1960}$ is 0.0829 °C, $r = 0.015$, $p = 0.924$; mean $GSATA_{1961-2000}$ is –0.0233 °C, $r = 0.319$, $p = 0.042$). According to the above division of cold and warm periods, the red noise of the global warming trend improves the correlation between GSATA and STD by its warm effect (here, mean $GSATA_{1881-1920}$ is –0.241 °C, cold than removed noise series, mean $GSATA_{1921-1960}$ is 0.984 °C, and mean $GSATA_{1961-2000}$ is 0.169 °C, $r_{1881-1920} = 0.225$, $p_{1881-1920} = 0.162$; $r_{1921-1960} = 0.123$, $p_{1921-1960} = 0.450$; $r_{1961-2000} = 0.389$, $p_{1961-2000} = 0.011$). Our STD results show a significant correlation with local winter temperature parameters (Fig. 4) and winter GSATA, especially in January. Removing red noise has a negative effect that weakens the observed periodicity (Fig. 3D) and makes higher frequency signals of GSATA less clear than those without the red noise (Figs. 3D, 3E and Tab. IV).

Wavelet spectra signal of GSATA was weaker than PDO, SSN, and STD. Strong amplitudes were observed in the band 2–20 year periodicities (Tab. IIIA). Alternate signals in this band are also present in some periods but absent in others, and the signal was clearly non-stationary. In some periods (1883–1889, 1895–1930, 1948–1962, 1977–1983 and 1988–2004), the signal around the 5 year cycle (4, 4.2, 5.2 y, Tab. IIIA) was stronger than others, while in other intervals, periodicities lower than 4 years (Tab. IIIA) had a stronger signal. The signal at 20.8 years is persistent during the entire period with lower intensity in the period 1916–1928. During the entire period, significant low frequency signal (62.5 y) is evident. Between 1880 and 2004, the wave crest and trough of tree ring scale-averaged wavelet power well fit to the fluctuation of average GSATA (Fig. 6C). Average tree rings and average GSATA showed consistent interdecadal changes, including a possible modulation in GSATA variance with a 20 year period. We also see the phenomena that GSATA (red noise has been removed) had a closer correlation with tree rings in 1900–1950 ($r = 0.228$, $p < 0.05$) than in 1951–2001 ($r = 0.210$, $p = 0.134$). GSATA's variation also demonstrates a uniform characteristic that cycles of relative warming and cooling can be observed in tree growth. Our analysis shows that GSATA has less effect on tree rings than PDO and SSN (Figs. 4, 6 and Tab. IV), perhaps because Chinese pine tree rings in this region are less responsive to temperature than to water regimes, which are mostly reflected by PDO and SSN (Fig. 4).

4. DISCUSSIONS

Several main points of our study relating the complexity of these Sun-Earth physical processes (either one or several operate together) are discussed as follows.

4.1. Relationships between tree rings and urban climate-environment factors

Urban expansion, especially industrial development, has heavily affected the growth of Chinese pines in our study area. These effects were recorded by tree-rings as early as the 1930s in Shenyang [55, 65]. Similar to the findings reported worldwide, the environmental pollution has become an important influence on tree rings after the 1960s [55, 65]. They found that there are significant linear correlations between Chinese pine tree-ring growth from Zhaoling Mausoleum and urban environmental variables (especially pollution) and that the environmental pollution of Shenyang can weaken the response of Chinese pine tree ring width to local climatic variables. Chinese pine chronologies show that tree rings are not only sensitive to local annual climate (such as mean air temperatures) but that they are also sensitive to global climatic variables, such as reflected by PDO and GSATA. Tree ring responses to the local and global climate can be further complicated or weakened by environmental factors. Although some signals and correlations are insignificant or weak, they reveal the influences of urban environmental factors on tree ring development. However, the precipitation in the region shows an uncertain relationship between the first semicentennial and the second semicentennial to Chinese pine tree rings in the last century (positive correlation in 1906–1950, negative correlation in 1951–1994). This is most likely due to precipitation, which is a more stochastic meteorological parameter than temperature. In addition the mean sensitivity of STD (0.1775) from Zhaoingling Mausoleum, located in the city, is less than in Fuling Mausoleum, located in a suburb (0.2265) [8, 9] and the Qianshan Mountains, located in natural sites (72 km to Shenyang, 0.2181) [8]. Qianshan Mountains Chinese pines and Fuling Mausoleum Chinese pines also have stronger responses to local climate than Chinese pines from Zhaoling Mausoleum [8]. These results suggest tree ring time series can reflect complex interactions

Table IV. Significant correlations between STD and PDO/GSATA (11 y running mean).

	Pearson correlation							
	May	Jun	Jul	Aug	Sep	Oct	Dec	Mean May–Oct
PDO (n = 100)	0.340**	0.286**	0.308**	0.269**	0.227*	0.224*		0.301**
GSATAr (n = 120)	0.193*						0.225*	

GSATAr is GSATA time series which the noise of global surface air temperature increasing trend has been removed; ** Correlation is significant at the 0.01 level (2-tailed); * Correlation is significant at the 0.05 level (2-tailed).

among local climate, urban environmental change, and their driving forces.

4.2. Effects of SSN on Tree Rings

Our results show that the influence of SSN on urban Chinese pine tree rings is opposite that of PDO, GSATA and local temperatures during the last century ($r_{1900-1950}$ = −0.184, $p_{1900\sim1950}$ = 0.196; $r_{1951-2001}$ = −0.264, $p_{1951-2001}$ = 0.061). The most active semicentennial time of SSN in the last 300 years, might be the period from 1951 to 2001, with an average annual SSN (74.6) nearly twice as large as (48.7) during 1900–1950. This phenomenon may suggest that the effect of heavy cosmic physical process, such as SSN, plays a dominate role in Sun-earth system because high SSN means high correlation between SSN and STD (Fig. 7A).

As an important factor of Sun-Earth system, SSN has a nearly 11n year periodic mode (n = 1, 2, 3, ...), and the near 11 year cycle is its dominant periodicity. We can see a continuous high amplitude for the periodicity near 11 years in almost the whole period from the wavelet spectrum plot, with several weak signals indicating short time intervals (highest near 1750, 1850 and 1950, approximately). Their common periodicity fluctuated from 6 to 16 years in the whole period. In these 3 periods, the SSN has a stronger influence on STD than in other periods. This result agrees with observations by others [52]. STD has a 20–23 year (≈11 y × 2) and a 11–13 year periodic band corresponding to SSN's 11n year periodicity. These results show that the nearly 11 year SSN periodic signal (Tab. III) has a significant influence on STD. Thus, the solar variations associated with SSN might be one of the important factors influencing annual tree growth. PDO, GSATA, local air temperature parameters and local precipitation also have a strong and significant 11n year periodic band and periodicity. For example, PDO is a 20–26 year periodic band (≈11 y × 2) and shows a 52 year periodicity (≈11 y × 5). GSATA shows a 20.8 year (≈11 y × 2) and a 62.5 year periodicity (≈11 y × 6). Local annual mean air temperature shows a 12.3 year (≈11 y with a 1.3 y lag) and a 49 year periodicity (≈11 y × 5), whereas local precipitation has a 3.5 year dominant periodicity, with three cycles complete at 10.5 years (≈11 y). The facts indicate that there are linkages between Sun-Earth systems.

We can see the three strongest Sun-causing bands in the tree ring chronology at 5–8, 11–13 and 20–23 year cycles, which correspond to SSN's three strong periodicities: 5.8 years (associated with 5.5 y, Second Harmonic Schwabe cycle of solar activity), 11.1 years (associated with 11 y, Schwabe cycle of solar activity) and 28.8 years (associated with 22 y, Hale cycle of solar activity). This suggests that significant periodicity (95%) of STD at 20 and 23 years, 11.1 and 11.5 years, 4.9 and 6.4 years represent a possible influence of the Hale, Schwabe and Second Harmonic Schwabe cycles of solar activity, respectively. Furthermore, our results suggest that parameters of other solar activities have great impact to terrestrial system, in addition to SSN. In one example, Schwabe cycle length of solar activity [48] has a stronger effect on climate than SSN. The STD's 49.8 year cycle (near the 0.05 confidence level) may be associated with the 57.9 year periodicity of SSN (correspond to Fourth harmonic of Suess cycle). These periodic signals are also observed and reported by others [18, 46, 47, 51, 52]. The important low frequency signals (> 70 y) reported in other studies [33, 51], such as the Gleissberg cycle of solar activity (often considered 88 year periodicity) that corresponds to our calculation of SSN's 96 year significant periodicity and Suess cycle (near 200 y) is not clearly detected in our STD. This might due to our detrending, which removed some low frequency signals. The centurial modulation of global and hemispheric change may also be distorted by volcanic effects, changes in greenhouse gases, and other causes [29]. These may lead to the weak response of tree growth to local climate (direct factors related to tree growth), reflected by low or broken frequency signals [29]. The main effect of SSN on the Sun-Earth system of these well known cycles has been clearly presented by Raspopov et al. [51] and other researchers. Our results agree with Nordemann et al. [47] that a consistent low frequency fluctuation of two time series and rhythmic variations of their correlation show a long term trend of tree rings that correspond to solar activity decreases and increases (Fig. 6A). SSN's frequencies increase during high SSN time and decrease during low SSN time [33]. The short periodicities of solar activities are optimum tree growth conditions [33, 68] suggesting that a plentiful correspondence of our short cycles between Chinese pine STD and SSN must be common phenomena. However, high SSN corresponding to short SSN periodicity has a stronger negative effect on Chinese pine tree ring width in Shenyang than low SSN corresponding to long periodicity (Fig. 7A). More than 80% tree–ring chronologies have negative correlation with SSN parameters, similar to the result analyzed by Zhou from 69 tree–ring data sets worldwide in 1998 [68]. The negative correlation between SSN and Chinese pine tree ring width from our study area was also detected in the Fuling Mausoleum [8, 9]. However, the *Picea jezoensis* tree–ring chronologies from Changbai mountains (41° 31'–42° 28' N, 127° 9'–128° 55' E) in northeast China developed by Yu [66] and the *Araucaria angustifolia*

tree–ring width time series from Brazil (27° 11' S, 51° 59' W) [52] have positive correlation with SSN (1900–1996). This suggests that the mechanism resulting in the positive or negative correlations between SSN and tree ring width is a complex series of interactions among individual site conditions of different regions (such as microenvironment and microclimate) and tree species. In addition, a lag of 0 years was obtained from cross correlation, which indicates that the growth of Chinese pine in Shenyang seems to immediately follow sunspot activity variability. The significance of ± 1–± 2 lag years suggests that a 1–2 year lag effect of SSN on tree rings exist.

4.3. Effects of PDO on tree rings

Our results agree with the research [14, 35] that PDO has a closer relation to tree rings during the growing season (May–October) than the cold season. The yearly relationship between PDO and tree rings from Shenyang is weaker than that of the seacoast of the northwest Pacific [35].This may be because its position is farther inland and the continental climate is dominant. Our research on Chinese pines in Fuling [8, 9] and Qianshan [8] also confirms the pattern above. Furthermore, the relationship between PDO and tree rings in warm PDO regimes is closer in cold PDO regimes [14] (Fig. 7B). STD results from all three study sites have a positive correlation with PDO. This result does not agree with the results reported for northeast Asia [35], but is consistent with the results of D'Arrigo et al. [17] from North American. We analyzed 13 chronologies of different tree species from Changbai mountains (closer to the Pacific than Shenyang) [66] and found that only the *Picea jezoensis* tree-ring chronologies have a negative correlation ($r = -0.227$, $p = 0.025$, $n = 98$) with PDO. This indicates that there are some uncertain physical processes affecting different scale ecological processes in the Land-Ocean system, and that different responses to the system occur. The common 4–6 year and 10–12 year periodic bands are scattered in several short periods (similar to Figs. 3A and 3C). Tree ring width variance corresponds well to PDO change (Fig. 6B), and the dominant wave crest and trough of the average tree ring width also has homothetic correspondence with high and low fluctuation of average PDO at a certain time. An abrupt PDO variance of a low amplitude period between 1965 and 1980 is seen when the wave of tree ring reaches at a relative low level in the plot. Both time series show consistent interdecadal changes, including a possible modulation in PDO variance with an approximate 20 year period. With the abrupt shift occurring in 1925, 1947 and 1977 [25] evident changes occurred in our Chinese pine tree rings. The key effects of 20 year periodicity agree with some of the present reports of climate reconstructions that are based on tree-rings from seacoast of the Pacific [14, 17, 25, 35]. They suggest that the PDO has been an important player in Pacific climate for at least the past a few centuries and that a 20–30 year cycle of climate regimes is normal [17, 25, 35]. Our results indicate that tree rings may present an evident response to a PDO mode when both STD and PDO show the strongest signals in the same band. However, there is a short lag time effect between PDO and STD due to the correlation coefficient at 0 year. That lag time is not significant, but the correlation is significant at 2 years lag.

4.4. Effects of GSATA on tree rings

Opposite to PDO, our STD shows a more significant response in cold GSATA regimes than in warm GSATA regimes in a nearly 40 year time interval. Warm PDO regimes in the western and central North Pacific Ocean typically exhibit cold surface temperature anomalies while the eastern Pacific exhibits above average temperatures, but the opposite condition exists during cool regimes [25]. Zhaoling Chinese pines are highly sensitive to cold surface temperature anomalies of the Northwest Pacific Ocean. We may further infer that since Shenyang is near the northernmost border where Chinese pines can normally grow [39], the Chinese pines here are not only sensitive to local cold temperature anomalies [8] but also to large scale cold temperature anomalies. We can agree that tree ring growth variations contain information on not only growing season temperatures but also winter and annual temperatures [51]. Although there are many the short (less than 8 y) cycles scattered in some time intervals, the GSATA's strongest band is 20–30 year cycles. The 20 and 23 year cycle (corresponding to Hale cycle) in our tree rings seems more closely associated with the strongest GSATA 20.8 year cycle than PDO's 26 year cycle and SSN's 28.8 year cycle. GSATA may be the number one cause of the 20 and 23 year cycles in tree rings. The signal variability at high frequencies embedded in STD and GSATA indicates that GSATA is a more complex interior abnormity of Earth system. It has sensitive and unstable characteristics, and probably had multi-scale influence from local climatic conditions as well as the variation and complexity of terrestrial and oceanic climate.

In general, many acknowledged oscillatory modes of Sun-Earth variables have been found in our study. As the crucial impetus of the global ecology system, solar activity has a great effect on PDO, GSATA and vegetation on the Earth. Tree growth is influenced simultaneously by SSN, PDO and GSATA, and showed a relative regular variation in our study. The periodic oscillation of SSN, PDO and GSATA has been recorded by tree rings of Chinese pine. SSN, PDO and GSATA have great effects on Chinese pine growth in our study area by influencing local climates, especially in the growing season (May–October). Our results also demonstrate that PDO and GSATA both change in a way consistent with fluctuations of SSN. It is possible that other climatic factors could be operating together, with the solar activity such as SSN variations. The signals of activities could have been amplified in the tree rings. The strongest complex effect is in 8–14 year and near 20–30 year bands. The 8–14 year band makes tree growth on a 11–13 year periodic band the strongest response, and the trees produce their second strongest wave signal near the 20–30 year periodic band. However, the responses of tree rings to climate-environment factors in high frequency signals may be the most difficult phenomena to explain. The high frequency signals, especially near the 3 year periodic band embedded in

tree rings also indicates the response of the annual growth of trees to the high frequency fluctuation of PDO, GSATA, SSN and regional factors (such as 3.5 y precipitation and 4.9 y temperature cycles) (Tab. IIIA). It may also indicate that local environmental conditions were extremely variable from extreme environmental events [28,29], such as from intense El Niño/La Niña events, abrupt volcanic activity, extreme drought, extreme cold, etc.

4.5. Comparisons with results derived elsewhere

On the other hand, SSN is not as precise indicator of interplanetary magnetic field, the factor really affecting terrestrial climate, as solar cycle length. Ogurtsov et al. [48] found mesoclimatic temperature of northern Fennoscandia recorded by tree rings has a closer correlation with solar cycle length than SSN. It is possible in our case that SSN has a weaker relationship with global temperature and local temperature than to water regimes. Among the tree rings tested, 4 recorded extreme temperature events (1783, 1884, 1912 and 1994) in summer in northwest Siberia (more than 6100 km to Shenyang) during recent 300 years [28], there are 1783, 1884 and 1992, 3 events corresponding to extremely narrow rings of our STD, and the 1912 event corresponding to a narrowing ring. This result indicates, that a key climatic factor affecting high latitude regional climate of north hemisphere, Siberian climatic variables (such as cold snap) heavily affected the climatic variables in Shenyang in the past. Therefore, like suburb region [9] Shenyang urban Chinese pine not only recorded local extreme climatic events, such as extreme cold and drought but also common large scale extreme climatic events, such as intense El Niño/La Niña events.

4.6. Assessing analytic routine

Correlation analysis provides readily accessible information about the dominant mode of linear responses between tree ring and Sun-Earth variables across time. It allows us to determine the common mesoclimatic factors making tree rings time series and environmental parameters time series comparable to each other. The disadvantage of correlation analysis, however, is that it is unable to render factors that are less frequent, time-dependent, and growth limiting. Wavelet analysis has unique advantage in our study as a powerful and effective tool. It can allow one to trace dynamics of basic periodicities. Wavelet transformation of a signal is a multi-parametric function in the general case. With the discrete Fourier transform spectrum analysis, the wavelet analysis disadvantage of less precision than spectrum analysis can be alleviated. The signal is analyzed in the frequency, in the Fourier transformation, whereas the wavelet allows analyses of signals in both frequency and time. Despite cross wavelet analysis being considered too imprecise to analyze two different physical processes at one time [44], it provides the pertinent information in our study when high precision is not necessary.

In this paper, we did not pursue the goal of studying a possible physical mechanism responsible for the influence of variability in solar activity, PDO, GSATA, and local climatic parameters. This mechanism is still unclear and is a subject for future research.

Acknowledgements: This work was funded by the National Natural Science Foundation of China Project 90411019 and 30600093, and the Foundation of Knowledge Innovation Program of Chinese Academy of Sciences (CAS) KZCX3-SW-43. We would like to thank Christopher Torrence and Gilbert P. Compto for wavelet analysis routine. We also thank to Mr. Chen Guoxu, Mrs. Liu Tiehong, Mr. Zheng Wei and Mr. Tian Wei, Urban Construction and Administration Bureau of Shenyang, China, Dr Li Liguang and Master Cui Jin, Institute of Atmospheric Environment, China Meteorological Administration, Shenyang, China for their pure-hearted help. Dr. Richard P. Guyette, Director of Missouri Tree Ring Lab at the University of Missouri, USA and Michael C. Stambaugh, Research Specialist in the Tree Ring Lab commented and edited this manuscript substantially. Ms. Christine Tew did helpful work for improving the English.

REFERENCES

[1] Barber V.A., Juday G.P., Finney B.P., Reduced growth of Alaskan white spruce in the twentieth century from temperature-induced drought stress, Nature 405 (2000) 668–673.

[2] Beer J., Siegenthaler U., Bonani G., Finkel R.C., Oeschger H., Sater M., Woelffi W., Information on past solar activity and geomagnetism from ^{10}Be in the camp century ice core, Nature 331 (1988) 675–679.

[3] Bond G., Kromer B., Beer J., Muscheler R., Evans M.N., Showers W., Hoffmann S., Lotti-Bond R., Hajdas I., Bonani G., Persistent solar influence on north Atlantic climate during the Holocene, Science 294 (2001) 2130–2136.

[4] Briffa K., Jones P.D., Basic chronology statistics and assessment, in: Cook E.R., Kairiukstis L.A. (Eds.), Methods of Dendrochronology, Kluwer Academic Publishing, Boston, 1990, pp. 137–152.

[5] Briffa K.R., Osborn T.J., Schweingruber F.H., Large-scale temperature inferences from tree rings: a review, Glob. Planet. Change 40 (2004) 11–26.

[6] Briffa K.R., Schweingruber F.H., Jones P.D., Osborn T.J., Shiyatov S.G., Vaganov A.E., Reduced sensitivity of recent tree-growth to temperature at high northern latitudes, Nature 391 (1998) 678–682.

[7] Brito-Castillo L., Díaz-Castro S., Salinas-Zavala C.A., Douglas A.V., Reconstruction of long-term winter stream flow in the Gulf of California continental watershed, J. Hydrol. 278 (2003) 39–50.

[8] Chen Z.J., Ancient Chinese Pine Tree-Ring-Recorded Climate Variations in Shenyang over the Past 300 Years, Ph.D. dissertation, Shenyang, Institute of Applied Ecology, Chinese Academy of Sciences, 2006 (in Chinese with English summary).

[9] Chen Z.J., He X.Y., Chen W., Shao X.M., Sun Y., Tao D.L. Solar activity, global surface air temperature anomaly and pacific decadal oscillation signals observed in urban outskirts tree ring records from Shenyang, China. Adv. Space Res. 38 (2006) 2272–2284.

[10] Cook E.R., Holmes R.L., Users manual for program ARSTAN, Laboratory of Tree-Ring Research, University of Arizona, Tucson, USA, 1986.

[11] Cook E.R., Kairiukstis L.A., Method of dendrochronology: application in environmental sciences, Kluwer Academic Publishers, Dordrecht, Holland, 1989.

[12] Cook E.R., A time series analysis approach to tree-ring standardization, Ph.D. dissertation, University of Arizona, Tucson, USA, 1985.

[13] Cook E.R., Meko D.M., Stockton C.W., A new assessment of possible solar and lunar forcing of the bidecadal drought rhythm in the western United States, J. Climate 10 (1997) 1343–1356.

[14] Cook E.R., Reconstructions of Pacific decadal variability from long tree-ring records, EOS: Transactions, American Geophysical Union 83 (19) Spring Meet. Suppl. (2002) S133.

[15] Crowley T., Causes of climate change over the past 1000 years, Science 289 (2000) 270–277.

[16] D'Arrigo R., Cook E.R., Wilson R.J., Allan R., Mann M.E., On the variability of ENSO over the past six centuries, Geophys. Res. Lett. 32 (2005) L03711.

[17] D'Arrigo R., Villalba R., Wiles G., Tree-ring estimates of Pacific decadal climate variability, Clim. Dynam. 18 (2001) 219–224.

[18] Damon P.E., Eastone C.J., Hughes M.K., Kalin R.M., Long A., Peristykh A.N., Secular variation of Δ^{14}C during the medieval solar maximum: a progress report, Radiocarbon 40 (1998) 343–350.

[19] Douglass A.E., Climatic cycles and tree growth, vol. II, Carnegie Institute of Washington Publications, Washington, DC, 1928.

[20] Dutilleul P., Till C., Evidence of periodicities related to climate and planetary behaviors in ring-width chronologies of Atlas cedar (*Cedrus atlantica*) in Marocco, Can. J. For. Res. 22 (1992) 1469–1482.

[21] Esper J., Cook E.R., Schweingruber F.H., Low-frequency signals in long tree-line chronologies for reconstructing past temperature variability, Science 295 (2002) 2250–2253.

[22] Friis-Christensen E., Lassen K., Length of the solar cycle – an indicator of solar activity closely associated with climate, Science 254 (1991) 698–700.

[23] Fritts H.C., Tree rings and climate, Academic Press Ltd., London, UK, 1976.

[24] Frölich C., Lean J., The sun's total irradiance cycles, trends and related climate change uncertainties since 1976, Geophys. Res. Lett. 97 (1998) 7579–7591.

[25] Gedalof Z., Mantua N.J., A multi-century perspective of variability in the Pacific Decadal Oscillation: new insights from tree rings and coral, 29 (24), Geophys. Res. Lett. (2002) 2204.

[26] Guo D.J., Wang X.D., Li X.C., Some debates upon the originationing region and mechanism of PDO, Chin. J. Trop. Meteorol. 19 suppl. (2003) 136–144 (in Chinese with English summary).

[27] Haigh J.D., Climate variability and the role of the Sun, Science. 294 (2001) 2109–2111.

[28] Hantemirov R.M., Gorlanova L.A., Shiyatov S.G., Extreme temperature events in summer in northwest Siberia since AD 742 inferred from tree rings. Palaeogeogr. Palaeocl. 209 (2004) 155–164.

[29] Hegerl G.C., Crowley T.J., Baum S.K., Kim K-Y, Hyde W.T. Detection of volcanic, solar and greenhouse gas signals in paleoreconstructions of Northern Hemispheric temperature, Geophys. Res. Lett. 30 (5) (2003) 1242.

[30] Holmes R.L., Computer-assisted quality control in tree-ring dating and measurement, Tree-Ring Bull. 43 (1983) 69–78.

[31] Huang H.Y., Jiang D.M., Lin Z.Q., Studied on the relation of tree-ring Cd-content with environmental pollution, Chin. Environ. Sci. 13 (1993) 11–16 (in Chinese with English summary).

[32] Huang J.Y., et al, Meteorological statistic and forecast methods, Meteorological Publishers, Beijing, China, 2000, pp. 232–233 (in Chinese).

[33] Huang L., Shao X.M., Precipitation variation in Delingha, Qinghai and solar activity over the last 400 years, Chin. Quaternary Sci. 25 (2005) 184–192 (in Chinese with English summary).

[34] Hughes M.K., Kelly P.M., Pilcher J.R., LaMarche V.C., Climate from tree rings, Cambridge University Press, 1982.

[35] Jacoby G., Solomina O., Frank D., Eremenko N., D'Arrigo R., Kunashir (Kuriles) oak 400-year reconstruction of temperature and relation to the Pacific Decadal Oscillation, Palaeogeogr. Palaeocl. 209 (2004) 303–311.

[36] Kocharov G.E., Ostryakov V.M., Peristykh A.N., Vasil'D V.A., Radiocarbon Content Variations and Maunder Minimum of Solar Activity, Sol. Phys. 159 (1995) 381–391.

[37] Kumar P., Foufoula-Georgiou E., Wavelet analysis for geophysical application, Rev. Geophys. 35 (1997) 385–412.

[38] Kurths J., Spiering C., Müller-Stoll W., Striegler U., Search for solar periodicities in miocene tree ring widths, Terra Nova 5 (1993) 359–363.

[39] Li S.X. et al., Flora Liaoningica, Liaoning science press, Shenyang, China, 1988 (in Chinese).

[40] Mann M.E., Bradley R.S., Hughes M.K., Northern hemisphere temperatures during the past millennium: inferences, uncertainties, and limitations, Geophys. Res. Lett. 26 (1999) 759–762.

[41] Mann M.E., Bradley R.S., Hughes M.K., Global scale temperature patterns and climate forcing over the past six centuries, Nature 392 (1998) 779–787.

[42] Mantua N.J., Hare S.R., The Pacific Decadal Oscillation, J. Oceanog. 58 (2002) 35–44.

[43] Mantua N.J., Hare S.R., Zhang Y., Wallace J., Francis R., A Pacific interdecadal climate oscillation with impacts on salmon production, Bull. Am. Meteorol. Soc. 78 (1997) 1069–1080.

[44] Maraun D., Kurths J., Cross wavelet analysis: significance testing and pitfalls. Nonlinear Proc. Geophys. 11 (2004) 505–514

[45] Mori Y., Evidence of an 11-year periodicity in tree-ring series from Formosa related to the sunspot cycle, J. Climatol. 1 (1981) 345–353.

[46] Murphy J.O., Australian tree-ring chronologies a proxy data for solar variability, Proceed. ASA 8 (1990) 292–297.

[47] Nordemann D.J.R., Rigozo N.R. Faria H.H., Solar activity and El-Niño signals observed in Brazil and Chile tree ring records, Adv. Space Res. 35 (2005) 891–896.

[48] Ogurtsov M.G., Kocharov G.E., Lindholm M., Merliäinen J., Eronen M., Nagovitsyn Y.U.A., Evidence of solar variation in tree-ring-based climate reconstructions, Sol. Phys. 205 (2002) 403–417.

[49] Park Y.I., Dallaire G., and Morin H., A method for multiple intra-ring demarcation of coniferous trees, Ann. For. Sci. 63 (2006) 9–14.

[50] Percival D.B., Walden A.T., Wavelet methods for time series analysis, Cambridge University Press, London, UK, 2000.

[51] Raspopov O.M., Dergachev V.A., Kolström T., Periodicity of climate conditions and solar variability derived from dendrochronological and other palaeoclimatic data in high latitudes, Palaeogeogr. Palaeocl. 209 (2004) 127–139.

[52] Rigozo N.R., Nordemann D.J.R., Echer E., Vieira L.E.A., Search for solar periodicities in tree-ring widths from Concordia (S.C., Brazil), Pure Appl. Geophys. 161 (2004) 221–233.

[53] Rind D., The Sun's role in climate variations, Science 296 (2002) 673–678.

[54] Rozas V., Dendrochronology of pedunculate oak (*Quercus robur* L.) in an old-growth pollarded woodland in northern Spain: establishment patterns and the management history, Ann. For. Sci. 62 (2005) 13–22.

[55] Shang H., Huang H.Y., Wang S.Q., Preliminary research on the reasons of declining and dying of palaeo-Chinese pine in Zhaoling Mausoleum, Shenyang, J. Shenyang Agri. Univ., 28 (1997) 39–43 (in Chinese with English summary).

[56] Shao X.M., Huang L., Liu H.B., Liang E.Y., Fang X.Q., Wang L.L., Reconstruction of precipitation variation from tree rings in recent 1000 years in Delingha, Qinhai. Sci. China. Ser. D. 34 (2004) 145–153.

[57] Shindell D.T., Schmidt G.A., Mann M.E., Rind D., Waple A., Solar forcing of regional climate change during the Maunder Minimum, Science 294 (2001) 2149–2152.

[58] Stuiver M., Quay P.D., Changes in atmospheric carbon-14 attributed to a variable sun, Science 207 (1980) 11–19.

[59] The Intergovernmental Panel on Climate Change, The third assessment report of the intergovernmental panel on climate change–climate change 2001: synthesis report. Published for IPCC Plenary XVIII Wembley, United Kingdom, Cambridge University, 2001, pp. 60.

[60] Torrence C., Compto G.P., A practical guide to wavelet analysis, B. Am. Meteorol. Soc. 79 (1998) 61–78.

[61] Wen K.G., Li B., Meng Q.N., China meteorological calamity grand ceremony: Liaoning rolls, Meteorological Publishers, Beijing, China, 2005 (in Chinese).

[62] Wigley T.M.L., Briffa K.R., Jones P.D., On the average value of correlated time series with applications in dendroclimatology and hydrometeorology, J. Clim. Appl. Meteorol. 23 (1984) 201–213.

[63] Wilson R.C., Hudson H.S., Sun luminosity variations in solar cycle 21, Nature 332 (1988) 810–812.

[64] Wu X.D. et al., Tree rings and climate change, Meteorological Publishers, Beijing, China, 1990 (in Chinese).

[65] Yu B., Huang H.Y., Variation of tree-ring in urban environment and its relation to industrial development. Chin. J. Appl. Ecol. 5 (1994) 72–77 (in Chinese with English summary).

[66] Yu D.P., Vegetation structure and dynamics of forest ecotones on northern aspect Changbai Mountain, Northeast China, Ph.D. dissertation, Institute of Applied Ecology, Chinese Academy of Sciences, Shenyang, China, 2004 (in Chinese with English summary).

[67] Zhang Y., Wallace J.M., Battisti D.S., ENSO-like interdecadal variability, J. Climate 10 (1997) 1004–1020.

[68] Zhou K., Butler C.J., A statistical study of the relationship between the solar cycle length and tree ring index values, J. Atmos. Terr. Phys. 60 (1998) 1711–1718.